Developmental Biology 321 (2008) 397–406

Contents lists available at ScienceDirect

Developmental Biology

journal homepage: www.elsevier.com/developmentalbiology

Reiterative roles for FGF signaling in the establishment of size and proportion of the zebrafish heart

Sara R. Marques [a,c], Yoonsung Lee [b], Kenneth D. Poss [b], Deborah Yelon [a,*]

[a] Developmental Genetics Program and Department of Cell Biology, Kimmel Center for Biology and Medicine, Skirball Institute of Biomolecular Medicine, New York University School of Medicine, New York, NY 10016, USA
[b] Department of Cell Biology, Duke University Medical Center, Durham, NC 27710, USA
[c] Graduate Program in Areas of Basic and Applied Biology, Universidade do Porto, 4050-465 Porto, Portugal

ARTICLE INFO

Article history:
Received for publication 7 April 2008
Revised 14 June 2008
Accepted 26 June 2008
Available online 4 July 2008

Keywords:
Zebrafish
Organogenesis
Heart development
Chamber formation
Ventricle
Atrium
FGF
Fgf8
acerebellar

ABSTRACT

Development of a functional organ requires the establishment of its proper size as well as the establishment of the relative proportions of its individual components. In the zebrafish heart, organ size and proportion depend heavily on the number of cells in each of its two major chambers, the ventricle and the atrium. Heart size and chamber proportionality are both affected in zebrafish *fgf8* mutants. To determine when and how FGF signaling influences these characteristics, we examined the effect of temporally controlled pathway inhibition. During cardiac specification, reduction of FGF signaling inhibits formation of both ventricular and atrial cardiomyocytes, with a stronger impact on ventricular cells. After cardiomyocyte differentiation begins, reduction of FGF signaling can still result in a deficiency of ventricular cardiomyocytes. Consistent with two temporally distinct roles for FGF, we find that increased FGF signaling induces a cardiomyocyte surplus only before cardiac differentiation begins. Thus, FGF signaling first regulates heart size and chamber proportionality during cardiac specification and later refines ventricular proportion by regulating cell number after the onset of differentiation. Together, our data demonstrate that a single signaling pathway can act reiteratively to coordinate organ size and proportion.

Introduction

Organ size is highly consistent among individuals of the same species. Similarly, the distinct subunits of an organ typically develop with the same relative proportions in each individual (Cook and Tyers, 2007; Hidalgo and ffrench-Constant, 2003). Comparison between different species suggests that organ size and proportion are highly dependent on cell number, although cell size can also influence organ dimensions (Auman and Yelon, 2004; Hidalgo and ffrench-Constant, 2003; Nijhout, 2003; Potter and Xu, 2001; Raff, 1996; Trumpp et al., 2001). Since organ size and proportion are critical for normal organ function, it is important to elucidate the mechanisms that regulate these parameters.

In the heart, each chamber serves as a distinct functional subunit, and it has long been recognized that the relative proportions of the cardiac chambers are constant under normal physiological conditions. All normal adult human hearts have essentially the same number of myocardial nuclei (Linzbach, 1960), suggesting that the cell number in each chamber does not vary either. However, little is known about how heart size and relative chamber proportion are coordinated during embryonic development. Specifically, it is unclear when these characteristics are acquired and if they are established simultaneously or separately during development. It also remains unknown whether heart size and chamber proportionality are established by the same signaling pathways or require different sets of signals.

Fibroblast growth factors (FGFs) are appealing candidates for signals that regulate the establishment of cardiomyocyte number. FGFs comprise a large family of secreted polypeptides thought to signal in a dose-dependent manner through receptor tyrosine kinases (Böttcher and Niehrs, 2005). Studies in a number of model organisms have implicated FGF signaling in cardiac specification (Zaffran and Frasch, 2002). In *Drosophila*, *heartless* (*Fgfr*) mutants completely lack the dorsal vessel (Beiman et al., 1996); this phenotype reflects roles of Fgfr both in mesoderm migration and in cardiac fate assignment (Michelson et al., 1998). FGF signaling is also required to establish cardiac identity in *Ciona*, and activation of FGF transcriptional targets causes the transformation of anterior tail muscle cells into heart cells (Davidson et al., 2006). In chick, FGF8 from the anterior endoderm seems to contribute to its ability to induce the expression of cardiac genes such as *NKX2-5* and *MEF2c* (Alsan and Schultheiss, 2002; Zhu et al., 1999). Fgf8 is also required to initiate *nkx2.5* expression in zebrafish (Reifers et al., 2000): *acerebellar* (*ace*, *fgf8*) mutants exhibit weak *nkx2.5* expression at early stages, although expression recovers as development proceeds. In mouse, it has been difficult to address the role of FGF signaling in cardiac specification, since *Fgf8*$^{-/-}$ (Sun et al.,

* Corresponding author. Fax: +1 212 263 7760.
E-mail address: yelon@saturn.med.nyu.edu (D. Yelon).

0012-1606/$ – see front matter © 2008 Elsevier Inc. All rights reserved.
doi:10.1016/j.ydbio.2008.06.033

1999) and *Fgfr1*$^{-/-}$ (Deng et al., 1994) mutant mice fail to complete gastrulation. However, consistent with the roles of FGFs in other species, *in vitro* studies have shown that *Fgfr1*$^{-/-}$ embryoid bodies fail to express cardiac genes and do not form contractile foci (Dell'Era et al., 2003).

FGFs may also contribute to the establishment of chamber proportion. Prior studies have pointed out that loss of FGF signaling causes more prominent defects in ventricles than it does in atria. In zebrafish, *fgf8* mutants exhibit small hearts with particularly notable reductions of the ventricle (Reifers et al., 2000). Additionally, mouse embryos hypomorphic for *Fgf8* (compound heterozygous *Fgf8*$^{neo/-}$) display a hypoplastic right ventricle and outflow tract along with a complex series of other cardiovascular abnormalities (Abu-Issa et al., 2002), as do tissue-specific knockout mice in which *Fgf8* is deleted from the anterior heart field, a territory giving rise to the ventricles and outflow tract (Ilagan et al., 2006; Park et al., 2006). Consistent with a differential effect of FGF signaling on ventricular and atrial cells, application of exogenous FGF2 or FGF4 in chick embryos promotes ventricular myosin heavy chain 1 (*VMHC1*) gene expression and decreases atrial myosin heavy chain (*AMHC1*) expression (Lopez-Sanchez et al., 2002). It is not yet clear whether this series of observations reflects a role of FGF signaling in setting the proper ratio of ventricular and atrial cell numbers.

Here, we test the hypothesis that FGF signaling influences both heart size and chamber proportionality through the establishment of the proper numbers of cardiomyocytes. Using the zebrafish heart as a model, we systematically evaluate the impact of FGF signaling on the number of ventricular and atrial cardiomyocytes by comparing the roles of FGF at early stages, during cardiac specification, and at later stages, following myocardial differentiation. We find that inhibition of FGF signaling during cardiac specification reduces the numbers of both types of cardiomyocytes, with the ventricular lineage exhibiting greater sensitivity over a longer period of time. Even after myocardial differentiation is underway, FGF inhibition remains able to affect the number of ventricular cardiomyocytes. Furthermore, we find that increased FGF signaling can induce excessive cardiomyocyte formation, but only prior to myocardial differentiation. Taken together, our results indicate that FGF signaling has reiterative roles in regulating heart size and chamber proportionality: early in development, FGF signaling helps to establish properly sized and proportioned cardiac progenitor pools, and, at later stages, FGF signaling continues to contribute to the regulation of ventricular cell number, potentially by controlling population maintenance or growth.

Materials and methods

Zebrafish

Zebrafish and embryos were maintained at 28.5 °C in standard laboratory conditions. In addition to wild-type fish, we used carriers of the *ace*^{ti282a} mutation (Reifers et al., 1998), carriers of the transgene *Tg (cmlc2:DsRed2-nuc*^{f2}*)* (Mably et al., 2003), and carriers of the transgene *Tg(hsp70:ca-fgfr1*^{pd3}*)*. The *Tg(hsp70:ca-fgfr1)* construct allows heat shock-inducible expression of a constitutively active form of *Xenopus* Fgfr1. A point mutation in the Fgfr1 kinase domain (K562E) results in autophosphorylation of the receptor in the absence of bound ligand (Neilson and Friesel, 1996). A transgenic line was generated by injecting 40 ng/mL of linearized, purified construct into zebrafish embryos at the 1-cell stage (Higashijima et al., 1997). We raised 200 injected embryos, screened the resulting fish for germline integration of the transgene, and established lines from successful founders. The *Tg(hsp70:ca-fgfr1)* construct also contains a cassette in which a 0.8 kb *dsred* coding sequence (plus SV40 polyA; BD Biosciences) is driven by the 0.7 kb zebrafish α-crystallin promoter (Kurita et al., 2003); this generates strong red fluorescence in the lens that is recognizable by 48 h post-fertilization (hpf) and persists throughout adulthood, thereby facilitating identification of transgenic fish in the F1 and subsequent generations.

Immunofluorescence and cell counting

To count cardiomyocytes in embryos carrying the transgene *Tg (cmlc2:DsRed2-nuc)*, we used immunofluorescence to detect DsRed in cardiomyocyte nuclei and atrial myosin heavy chain (Amhc) in atrial cells, as described previously (Schoenebeck et al., 2007). Embryos were compressed under a cover slip and photographed with a Zeiss Axiocam on Zeiss M2Bio and Axioplan microscopes. Zeiss AxioVision 3.0.6 software and Adobe Photoshop Creative Suite were used to process images before counting fluorescent nuclei in each chamber. When comparing sets of cell number data, Student's *t*-test (homocedastic, two-tail distribution) was used to determine if the differences between the means of data sets were statistically significant.

In situ hybridization

Anti-sense *amhc*, *vmhc*, *cmlc2*, *pea3* and *tbx5* probes were used for in situ hybridization as previously described (Berdougo et al., 2003; Brown et al., 1998; Yelon et al., 1999, 2000). Embryos were examined on a Zeiss Axioplan microscope and photographed with a Zeiss Axiocam. Zeiss AxioVision 3.0.6 software and Adobe Photoshop Creative Suite were used to process images. Areas of gene expression were measured using Image J (http://rsb.info.nih.gov/ij/index.html). When comparing expression area data, Student's *t*-test (homocedastic, two-tail distribution) was used to determine if the differences between the means of data sets were statistically significant.

SU5402 treatments

A 1 mM stock of SU5402 (Calbiochem) in DMSO was diluted to a working concentration of 12.5 μM in E3 medium (Nusslein-Volhard and Dahm, 2002), a concentration of SU5402 that causes a strong reduction but does not completely abolish FGF signaling. Additional experiments utilized a working concentration of 9 μM SU5402, a concentration sufficient to induce circulation defects and pericardial edema. Up to 10 embryos were treated for discrete periods of time in glass vials in a final volume of 1 mL. Vials were kept in a nutator in the dark at 28.5 °C. After treatment, embryos were washed in 50 mL of E3 medium and placed in new glass vials with fresh E3 medium. Control embryos were treated with a corresponding dilution of DMSO in E3 medium.

In order to address the effectiveness of SU5402, we analyzed the expression of the Fgf signaling pathway target gene *polyoma enhancer activator 3* (*pea3*), which is known to be abolished with higher doses of SU5402 (Roehl and Nüsslein-Volhard, 2001). The concentration of SU5402 used in our experiments strongly reduces *pea3* expression as soon as 30 min after exposure, and *pea3* expression is restored 2 h after SU5402 removal (SRM and DY, unpublished data). The length of this recovery period is similar to that previously reported for SU5402 by others (Crump et al., 2004; Maroon et al., 2002; Nechiporuk et al., 2005).

Heat shock conditions

Embryos from outcrosses of fish heterozygous for *Tg(hsp70:ca-fgfr1)* were kept at 28.5 °C and heat shocked at desired stages. Embryos were placed in 40 mL of embryo medium in a Petri dish on top of a covered heat block for 20 min at 37 °C. Following heat shock, transgenic embryos were identified by their elongated body morphology at the 19-somite or 21-somite stages or by the expression of the α-*crystallin:dsred* cassette in the lens at 48 hpf. Heat shocked non-transgenic sibling embryos served as controls.

Results

acerebellar mutants have small hearts with disproportionately reduced ventricles

Prior studies have shown that the zebrafish mutation *acerebellar* (*ace*^{ti282a}), a loss-of-function allele of *fgf8*, causes formation of undersized hearts with a particular reduction of the ventricle (Reifers et al., 1998, 2000). Wild-type hearts display characteristically curved and expanded chambers (Fig. 1A), whereas *ace* mutant hearts resemble immature, linear tubes (Fig. 1B). Cardiomyocyte cell shape abnormalities contribute to the dysmorphic nature of the *ace* mutant heart (SRM and DY, unpublished data): in particular, ventricular cardiomyocytes in *ace* mutants do not undergo the regionalized processes of cellular enlargement and elongation that usually accompany chamber emergence (Auman et al., 2007). Since normal chamber emergence requires blood flow (Auman et al., 2007), this phenotype is consistent with the failure of *ace* mutants to establish circulation (Reifers et al., 2000). However, it is unclear whether the chamber morphology defects in *ace* mutants simply reflect errors in morphogenesis or may also be due to anomalies in cell number.

To determine whether the small dimensions of *ace* mutant hearts are related to reduced cell numbers, we counted ventricular and atrial cardiomyocytes in wild-type and *ace* mutant embryos. At 48 h post-fertilization (hpf), wild-type hearts typically contain approximately 30% more ventricular cells than atrial cells (Fig. 1C; Supplemental Table 1). In *ace* mutant hearts, total cell number is significantly reduced (Fig. 1C; Supplemental Table 1). Both ventricular and atrial cardiomyocyte populations are affected, but the ventricular cell loss is more dramatic than the atrial cell loss (Fig. 1C; Supplemental Table 1). As a result, *ace* mutant hearts typically contain approximately 50% more atrial cells than ventricular cells (Fig. 1C; Supplemental Table 1). Thus, in *ace* mutants, cell number deficiencies underlie abnormalities in both organ size and chamber proportionality.

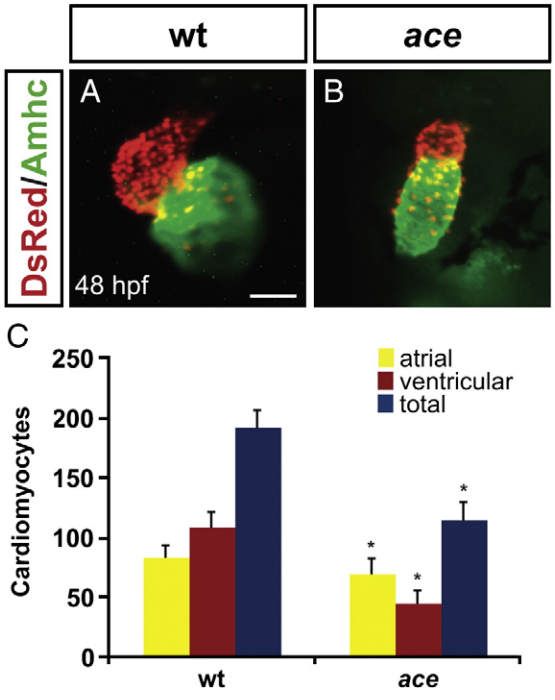

Fig. 1. *ace* mutant embryos have reduced numbers of both ventricular and atrial cardiomyocytes. (A, B) Frontal views of hearts from wild-type (A) and *ace* mutant (B) embryos at 48 hpf; immunofluorescence detects DsRed (red) in all cardiomyocyte nuclei and atrial myosin heavy chain (Amhc; green) in atrial cells. (A) In a wild-type heart, the ventricle (red) and atrium (green) exhibit typical looping and expansion. (B) In an *ace* mutant heart, the chambers are unlooped and small, with a particularly apparent reduction of the ventricle. Scale bar represents 50 μm; both images are shown at the same magnification. (C) Quantification of cardiomyocytes at 48 hpf reveals that the numbers of both ventricular and atrial cells are significantly decreased in *ace* mutants, with ventricular cell number being more affected then atrial cell number. Graph indicates mean and standard deviation for each data set; asterisks indicate statistically significant differences relative to wild-type ($p<0.005$, Student's *t*-test). $n=13$ for wild-type, and $n=19$ for *ace* mutants; see also Supplemental Table 1.

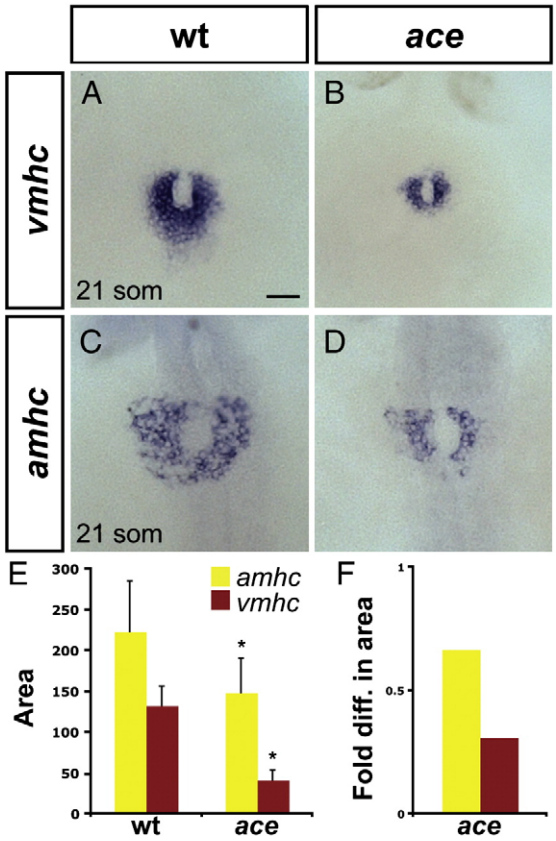

Fig. 2. Chamber disproportionality is evident prior to heart tube assembly in *ace* mutants. (A–D) In situ hybridization depicts expression of *vmhc* (A, B) and *amhc* (C, D) at the 21-somite stage; dorsal views, anterior to the top. Scale bar represents 50 μm; all images are shown at the same magnification. (A) In wild-type embryos, *vmhc* is expressed in a ring of ventricular cardiomyocytes just prior to heart tube extension. (B) In *ace* mutant embryos, the population of *vmhc*-expressing cells is clearly reduced ($n=14/15$). (C) *amhc* is expressed in a ring of atrial cardiomyocytes, surrounding the ventricular cardiomyocytes. (D) The population of *amhc*-expressing cells is also reduced in *ace* mutant embryos ($n=11/13$). (E) Graph indicates mean and standard deviation of areas of expression (in μm^2) of *amhc* and *vmhc* in wild-type and *ace* mutant embryos. Asterisks indicate statistically significant differences relative to wild-type ($p<0.005$, Student's *t*-test). $n\geq 10$ for all data sets; see also Supplemental Table 2. (F) Graph indicates fold difference in mean areas of gene expression relative to wild-type.

Chamber disproportionality is evident prior to heart tube assembly in ace mutants

The overall reduction in cardiomyocyte number observed in *ace* mutants is likely to reflect early defects in cardiac specification, since expression of several pre-cardiac markers fails to initiate properly in the *ace* mutant lateral plate mesoderm (LPM) (Reifers et al., 2000). However, these data do not resolve whether Fgf8 affects ventricular and atrial lineages simultaneously. To evaluate ventricular and atrial cardiomyocyte populations in the LPM, we examined expression of the earliest known chamber-specific genes *ventricular myosin heavy chain* (*vmhc*) and *atrial myosin heavy chain* (*amhc*) at the 21-somite stage. At this timepoint, the two bilateral cardiac fields have migrated toward the midline where they fuse to form a ring of cardiomyocytes (Berdougo et al., 2003; Yelon et al., 1999). Even at this early stage, it is clear that *ace* mutants exhibit diminished populations of both

ventricular cells (Figs. 2A, B) and atrial cells (Figs. 2C, D). Furthermore, quantification of the areas of *vmhc* and *amhc* expression reveals that the effects on the ventricular population are more striking than the effects on the atrial population (Figs. 2E, F; Supplemental Table 2). Since the size and organization of individual *vmhc*-expressing and *amhc*-expressing cells do not appear to be altered in *ace* mutants at this stage, the areas of *vmhc* and *amhc* expression suggest that *ace* mutants have only one-third of the number of *vmhc*-expressing cells and two-thirds of the number of *amhc*-expressing cells seen in wild-type embryos (Fig. 2F). Together, our data reveal that the influence of

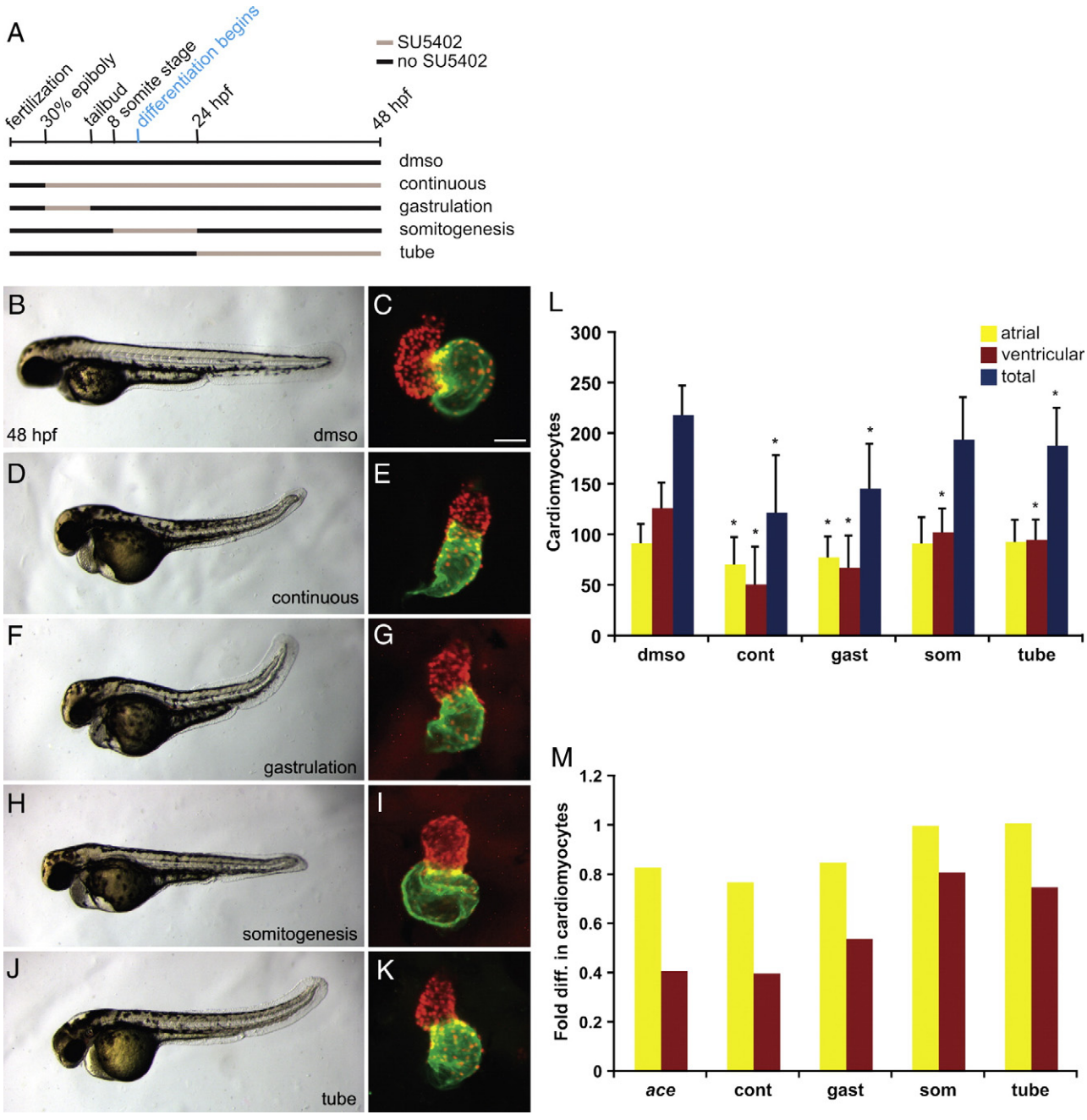

Fig. 3. Transient reduction of FGF signaling leads to differential reduction of cardiomyocyte numbers. (A) Schematic depicts the transient periods of FGF signaling inhibition caused by addition and removal of SU5402. Black lines represent time intervals with normal FGF signaling, and tan lines represent intervals of SU5402 treatment. Control embryos were treated only with DMSO, "continuous" SU5402 treatment extended from 30% epiboly (3 hpf) until 48 hpf, "gastrulation" treatment began at 30% epiboly and ended at the tailbud stage (10 hpf), "somitogenesis" treatment began at the 8-somite stage (13 hpf) and ended at 24 hpf, and "tube" treatment extended from 24 hpf to 48 hpf. (B–K) Representative 48 hpf embryos, lateral views, exhibiting morphology resulting from each type of SU5402 treatment, coupled with respective frontal views of hearts in which immunofluorescence detects DsRed (red) in all cardiomyocyte nuclei and Amhc (green) in atrial cells, as in Fig. 1. Scale bar represents 50 μm; all images of hearts are shown at the same magnification. Embryos treated continuously or during gastrulation occasionally exhibited severe tail truncations characteristic of higher SU5402 concentrations (Griffin and Kimelman, 2003); severely truncated embryos were excluded from quantification of cardiomyocytes. The concentration of SU5402 used did not induce nonspecific apoptosis, as indicated by TUNEL (SRM and DY, unpublished results). (L) Quantification of cardiomyocytes at 48 hpf after each type of SU5402 treatment. Graph indicates mean and standard deviation for each data set; asterisks indicate statistically significant differences relative to DMSO-treated controls ($p<0.005$, Student's *t*-test). Note that the total number of cardiomyocytes following somitogenesis treatment is also significantly different from the control number, although with a larger *p* value ($p<0.01$). (M) Graph indicates fold difference in mean values relative to wild-type for *ace* mutant embryos and embryos treated with SU5402. $n=33$ for DMSO, $n=8$ for continuous treatment, $n=28$ for gastrulation treatment, $n=28$ for somitogenesis treatment, and $n=22$ for tube treatment; see also Supplemental Table 3.

fgf8 on both ventricular and atrial lineages begins at early stages, prior to heart tube assembly.

FGF signaling influences both the ventricular and atrial lineages during gastrulation stages

We wondered whether the impact of Fgf8 on cardiomyocyte numbers could begin as early as gastrulation stages, when *fgf8* transcripts accumulate in a dorsoventral gradient at the margin of the embryo, with the highest levels of *fgf8* expression positioned dorsally (Fürthauer et al., 1997; Reifers et al., 1998). Fate maps of the zebrafish blastula indicate that myocardial progenitors reside in a region of the lateral margin that overlaps with the *fgf8* expression domain (Keegan et al., 2004; Stainier et al., 1993). Furthermore, ventricular and atrial progenitors are spatially organized prior to gastrulation, with ventricular progenitors located more dorsally and atrial progenitors located more ventrally (Keegan et al., 2004). Thus, myocardial progenitors, particularly ventricular progenitors, are likely to be exposed to Fgf8 during gastrulation.

To test whether FGF signaling during gastrulation is required for production of the proper number of cardiomyocytes, we treated embryos with 12.5 μM SU5402, a specific inhibitor of FGFR tyrosine kinase activity (Mohammadi et al., 1997). Since the effects of SU5402 are rapid and reversible (see Materials and methods), adding and removing the compound at different stages allowed us to create a transient period of attenuated FGF signaling and evaluate its impact on cardiomyocyte number at 48 hpf (Fig. 3A). We compared embryos exposed to SU5402 continuously (from 30% epiboly to 48 hpf; Figs. 3A, D, E) to embryos exposed only during gastrulation (from 30% epiboly to tailbud stage; Figs. 3A, F, G). Embryos continuously exposed to SU5402 morphologically resemble *ace* mutants (Fig. 3D; SRM and DY, unpublished data): they lack the midbrain–hindbrain boundary and exhibit a shortened body axis, consistent with roles of FGF in brain, trunk, and tail development (Griffin and Kimelman, 2003). Additionally, hearts of embryos continuously exposed to SU5402 resemble *ace* mutant hearts morphologically and in terms of cell number (Figs. 1B, C and Figs. 3E, L, M; Supplemental Table 3). The hearts of embryos treated during gastrulation appear slightly larger than the hearts of continuously treated embryos (Figs. 3E, G), though they are still small and dysmorphic relative to wild-type (Fig. 3C). Consistent with their morphology, the hearts of embryos treated during gastrulation exhibit significant deficiencies in both ventricular and atrial cell numbers (Figs. 3L, M; Supplemental Table 3). It is noteworthy that both continuous treatment and treatment during gastrulation reduce ventricular cell number more significantly then atrial cell number, as seen in *ace*. The same trend is seen in embryos exposed to 9 μM SU5402 during gastrulation (Supplemental Table 4). Comparing the effectiveness of the different SU5402 treatments, we observe similar effects on atrial cell number in *ace* mutants, embryos exposed to SU5402 continuously, and embryos exposed to SU5402 during gastrulation (Fig. 1C and Figs. 3L, M). In contrast, ventricular cell number appears more affected in *ace* mutants and in embryos treated continuously with SU5402 than it is in embryos treated only during gastrulation (Figs. 1C and 3L, M). Taken together, our results indicate that FGF signaling during gastrulation stages plays an important role in promoting the formation of both ventricular and atrial cardiomyocytes.

A continuing influence of FGF signaling on ventricular cardiomyocyte number

While FGF signaling during gastrulation clearly has a potent effect on cardiomyocyte formation, our data also imply that the impact of FGF signaling on the ventricular lineage extends beyond these stages, since we find that continuous treatment with SU5402 has a stronger effect than treatment only during gastrulation on the number of ventricular cardiomyocytes (Figs. 3L, M). The locations of myocardial progenitors after gastrulation continue to correlate with the locations of *fgf8* expression, with particular proximity of ventricular progenitors to sources of *fgf8* (Reifers et al., 2000). Following gastrulation, myocardial progenitors integrate into the LPM, with ventricular progenitors located more medially than atrial progenitors (Schoenebeck et al., 2007). Robust expression of pre-cardiac markers like *nkx2.5* begins around the 6–8-somite stage, at which time *fgf8* expression is medially adjacent to and overlapping with the pre-cardiac portion of the LPM (Reifers et al., 2000). Terminal differentiation of cardiomyocytes begins around the 13-somite stage, when these cells initiate expression of myocardial markers like *cmlc2* (Yelon et al., 1999). Heart tube assembly then facilitates the merger of bilateral cardiomyocyte populations and creates discrete domains of ventricular and atrial cardiomyocytes within the linear tube by 24 hpf (Auman et al., 2007). Even after myocardial differentiation is underway, *fgf8* expression persists in ventricular cells and is apparent in the ventricular portion of the heart tube (Reifers et al., 2000). Thus, the *fgf8* expression pattern suggests multiple opportunities for FGF signaling to influence ventricular development.

To test whether FGF signaling is required for cardiomyocyte formation after gastrulation stages, we examined the effects of inhibiting FGF signaling during somitogenesis stages (from the 8-somite stage to 24 hpf; hereafter referred to as somitogenesis treatment) and after the heart tube has formed (from 24 hpf to 48 hpf; hereafter referred to as tube treatment) (Fig. 3A). Embryos exposed to SU5402 during somitogenesis and tube stages show disorganized development of tail somites (Figs. 3H, J), consistent with reported roles for FGF in posterior myogenesis (Hamade et al., 2006).

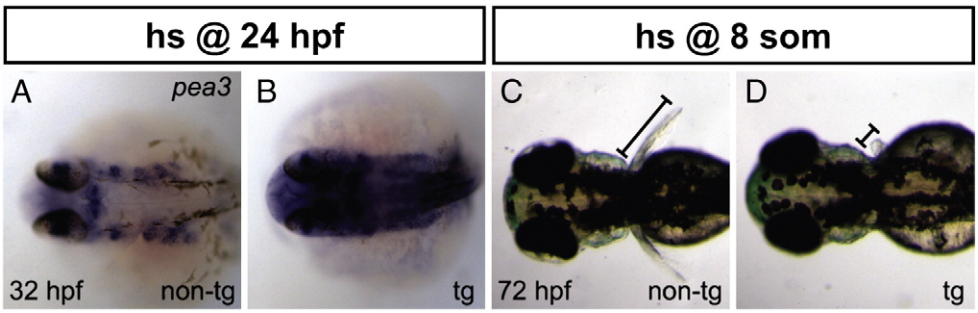

Fig. 4. Heat shock of *Tg(hsp70:ca-fgfr1)* embryos causes ectopic FGF signaling and perturbs pectoral fin development. (A, B) In situ hybridization depicts *pea3* expression at 32 hpf; dorsal views, anterior to the left. (A) After heat shock at 24 hpf, non-transgenic (non-tg) embryos show a wild-type restriction of *pea3* expression to specific regions, including the midbrain–hindbrain boundary and the pharyngeal pouches. (B) In contrast, heat shock of transgenic (tg) embryos causes strong and ectopic expression of *pea3*. (C, D) Dorsal views at 72 hpf of embryos after heat shock at the 8-somite stage. (C) Non-transgenic embryos exhibit pectoral fins of normal length (bar). (D) Transgenic embryos lack at least one pectoral fin, as shown here (n=14/50), or have two small fins (n=31/50).

Additionally, somitogenesis treatment results in tubular ventricles with expanded atria (Fig. 3I) and causes a significant loss of ventricular cardiomyocytes (Figs. 3L, M; Supplemental Table 3); however, atrial cell number is unchanged. A similar, though not statistically significant, trend is observed in embryos exposed to 9 μM SU5402 during somitogenesis stages (Supplemental Table 4). Tube treatment results in mild defects in cardiac looping and chamber morphology (Fig. 3K) and also causes a significant reduction in ventricular cell number (Figs. 3L, M, Supplemental Table 3); like somitogenesis treatment, tube treatment does not affect atrial cell number. Together, these results reveal that FGF signaling has a continuing influence on ventricular cell number that extends well beyond its role during gastrulation.

Ectopic FGF signaling prior to terminal differentiation creates a cardiomyocyte surplus

Our loss-of-function data point to a general correlation between levels of FGF signaling and the number of cardiomyocytes generated. Prior studies have shown that ectopic FGF signaling is sufficient to induce cardiac gene expression; for example, FGF8-soaked beads induce *nkx2.5* in chick (Alsan and Schultheiss, 2002) and zebrafish (Reifers et al., 2000). However, it is not known whether induction of gene expression by ectopic FGF signaling results in a surplus of cardiomyocytes. To test this hypothesis, we employed transgenic embryos carrying *Tg(hsp70:ca-fgfr1)*, which allows heat-inducible expression of a constitutively active form of Fgfr1 (see Materials and

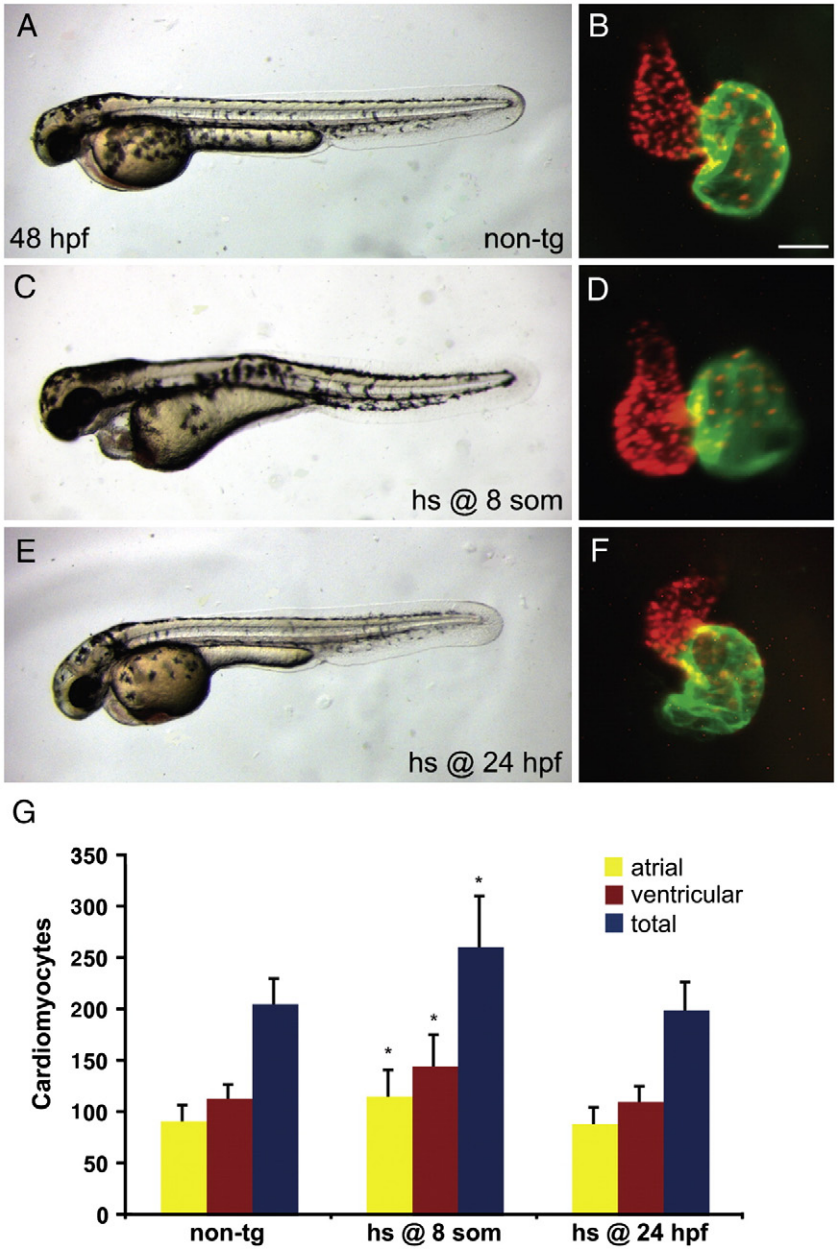

Fig. 5. Increased FGF signaling prior to terminal differentiation induces a surplus of cardiomyocytes. (A–F) Representative non-transgenic (A) or *Tg(hsp70:ca-fgfr1)* (C, E) sibling embryos at 48 hpf, lateral views, exhibiting morphology resulting from heat shock at the 8-somite stage (C) or at 24 hpf (E), coupled with respective frontal views of hearts in which immunofluorescence detects DsRed (red) in all cardiomyocyte nuclei and Amhc (green) in atrial cells, as in Fig. 1. Scale bar represents 50 μm; all images of hearts are shown at the same magnification. (C, D) Although heat shock at the 8-somite stage causes pericardial edema (C) and dysmorphic cardiac chambers (D), heat shock at 24 hpf does neither (E, F). (G) Quantification of cardiomyocytes at 48 hpf reveals that increased FGF signaling causes a significant cardiomyocyte surplus only in embryos heat shocked at the 8-somite stage. Graph indicates mean and standard deviation for each data set; asterisks indicate statistically significant differences relative to non-tg controls ($p<0.005$, Student's *t*-test). $n=24$ for non-tg, $n=18$ for heat shock at the 8-somite stage, and $n=14$ for heat shock at 24 hpf; see also Supplemental Table 5.

methods). Heat shock of transgenic embryos rapidly induces high levels of FGF signaling throughout the embryo: ectopic and robust expression of the FGF pathway target gene *pea3* begins as early as 2 h after heat shock and is maintained for at least 8 h (Figs. 4A, B; SRM, YL, KDP, and DY, unpublished data).

We increased FGF signaling through heat shock of transgenic embryos at the beginning of each time interval analyzed with SU5402 treatment. First, we found that heat shock of transgenic embryos at 30% epiboly results in severely dorsalized embryos consistent with what has been previously reported for *fgf8* RNA injection (Fürthauer et al., 1997), preventing us from analyzing ventricular and atrial cell numbers at 48 hpf (SRM, YL, KDP, and DY, unpublished data). In contrast, heat shock of transgenic embryos at the 8-somite stage does not grossly disrupt embryonic axis formation (Figs. 5A, C), although it does cause body elongation (Fig. 5C), yolk extension abnormalities (Fig. 5C), and pectoral fin (forelimb) defects ranging from loss of fins to reduction of fin size (Figs. 4C, D). Heat shock at the 8-somite stage also results in severe pericardial edema (Fig. 5C) and elongated cardiac chambers (Figs. 5B, D). By counting ventricular and atrial cardiomyocytes at 48 hpf, we found that activation of FGF signaling at the 8-somite stage can lead to an approximately 25% increase in the numbers of both ventricular and atrial cells (Fig. 5G; Supplemental Table 5).

The cardiomyocyte surplus caused by heat shock at the 8-somite stage is evident even a few hours following overexpression of the constitutively active receptor: heat shocked embryos exhibit posterior expansions of *cmlc2*, *vmhc*, and *amhc* expression within the LPM prior to heart tube assembly (Figs. 6A–F). Based on the observed expansion, it is interesting to consider that increased FGF signaling may recruit cells into the myocardial lineage from positions posterior to the heart field. Coincident with the appearance of enlarged heart fields in embryos heat shocked at the 8-somite stage, we also observe reduction of the pectoral fin fields, bilateral zones of *tbx5* expression located posterior to the heart fields within the LPM (Figs. 6G, H) (Ahn et al., 2002; Begemann and Ingham, 2000). This loss of pectoral fin precursors is consistent with the observed reduction or absence of pectoral fins at later stages (Figs. 4C, D) and suggests the possibility that ectopic FGF signaling can transform pectoral fin progenitors into myocardial progenitors.

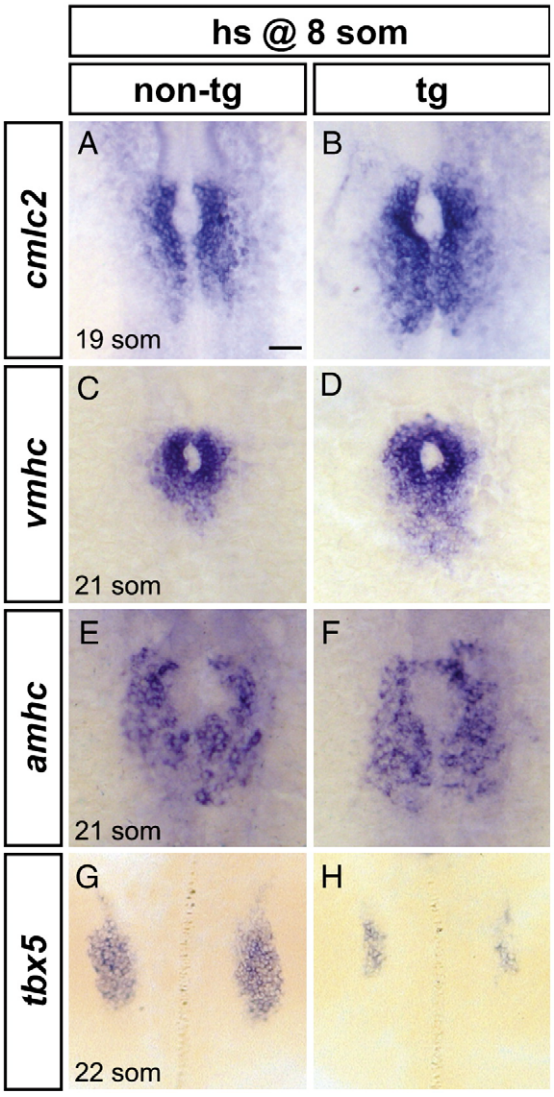

Fig. 6. Increased FGF signaling enhances formation of cardiomyocyte populations and inhibits formation of the pectoral fin field. (A–H) In situ hybridization depicts expression of *cmlc2*, *vmhc*, *amhc* and *tbx5* at the 19-somite or 21-somite stage in non-transgenic (A, C, E, G) and *Tg(hsp70:ca-fgfr1)* (B, D, F, H) sibling embryos after heat shock at the 8-somite stage; dorsal views, anterior to the top. Scale bar represents 50 μm; all images are shown at the same magnification. (A, B) Ectopic FGF signaling leads to a posterior expansion of *cmlc2*-expressing cardiomyocytes (n=30/37). (C, D) Ectopic FGF signaling leads to a posterior expansion of *vmhc*-expressing ventricular cardiomyocytes (n=16/19). (E, F) Ectopic FGF signaling leads to a mild posterior expansion of *amhc*-expressing atrial cardiomyocytes (n=8/10). (G, H) Ectopic FGF signaling leads to reduction of the pectoral fin field, as demarcated by *tbx5* expression (n=18/18).

Loss of FGF signaling does not enlarge the pectoral fin field

The notion that ectopic FGF signaling may recruit cells from the forelimb field into the heart field suggests that endogenous FGF signaling might play a role in distinguishing the developmental potential of the heart and forelimb fields. In this scenario, loss of FGF signaling would cause expansion of the forelimb field at the expense of the heart field. However, *ace* mutants develop normal pectoral fins (Reifers et al., 1998), and *fgf24* mutants display normal *tbx5* expression (Fischer et al., 2003) at 24 hpf. It has also been reported that exposure to SU5402 from the 1-somite stage until the 23-somite stage does not perturb *tbx5* expression (Mercader et al., 2006). However, prior studies have not addressed whether loss of FGF signaling during gastrulation stages could result in pectoral fin field expansion.

We examined *tbx5* expression in the forelimb fields and in the pectoral fins of embryos treated with SU5402 continuously, during gastrulation, or during somitogenesis (Fig. 7). None of these treatments causes expansion of the area of *tbx5* expression in the pectoral fin field at 20 hpf (Figs. 7A, C, E, G). Pectoral fin size at 48 hpf also appears normal in embryos treated with SU5402 during gastrulation (Fig. 7F) or somitogenesis (Fig. 7H), although fin morphology appears variably aberrant following somitogenesis treatment. Embryos continuously treated with SU5402 lack pectoral fins at 48 hpf (Fig. 7D), consistent with a role for Fgf24 in pectoral fin development after 24 hpf (Fischer et al., 2003; Mercader et al., 2006). Thus, while loss of FGF signaling results in a reduction of the heart field, we cannot detect a concomitant expansion of the forelimb field. Taken together, these results do not support a role for FGF signaling in regulating a decision between heart and forelimb fates.

Induction of ectopic FGF signaling after heart tube assembly does not affect cardiomyocyte number

Generation of a cardiomyocyte surplus by ectopic FGF signaling suggests that some developmental plasticity remains within the organ fields of the LPM during somitogenesis stages. We wondered whether this plasticity is maintained after myocardial differentiation begins. To address this, we chose to induce ectopic FGF signaling via heat shock of *Tg(hsp70:ca-fgfr1)* embryos at 24 hpf. Like heat shock at the 8-somite stage, heat shock of transgenic embryos at 24 hpf does not disturb general embryonic morphology (Fig. 5E). However, in contrast

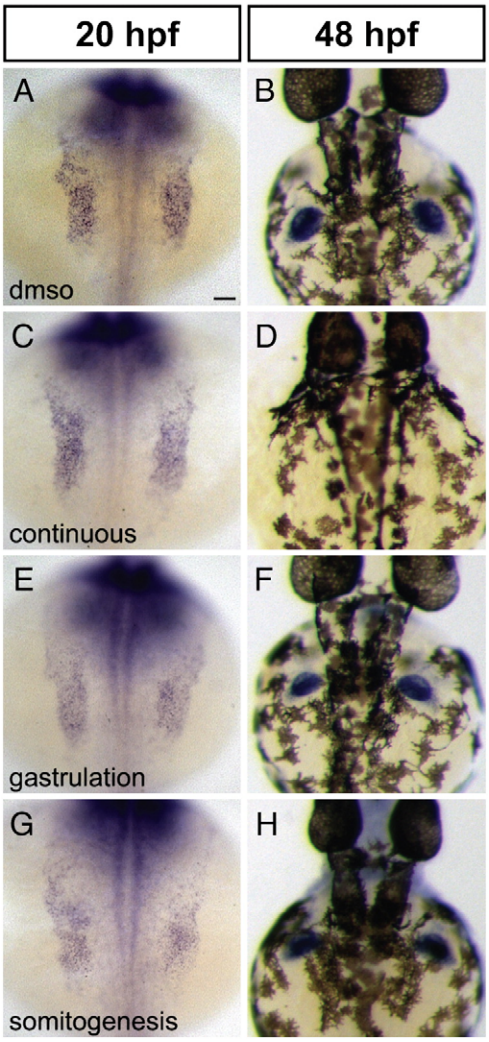

Fig. 7. Reduction of FGF signaling does not expand the forelimb field. (A–H) In situ hybridization depicts expression of *tbx5* at 20 hpf (A, C, E, G) and 48 hpf (B, D, F, H); dorsal views, anterior to the top. Scale bar represents 50 μm; all images are shown at the same magnification. (A–D) Compared to control embryos treated only with DMSO (A, B), embryos exposed to continuous SU5402 treatment exhibit normal areas of *tbx5* expression in the pectoral fin fields at 20 hpf (C; $n=8/8$) but lack pectoral fins at 48 hpf (D; $n=15/15$). (E, F) Embryos treated with SU5402 during gastrulation exhibit normal areas of *tbx5* expression in the pectoral fin fields at 20 hpf ($n=16/16$) and normal pectoral fins at 48 hpf ($n=18/18$). (G, H) Embryos treated with SU5402 during somitogenesis do not display increased areas of *tbx5* expression in the pectoral fin fields at 20 hpf ($n=9/9$) and do not have detectable defects in pectoral fin size at 48 hpf ($n=15/16$), although fin morphology varies between treated embryos. It is noteworthy that the level of *tbx5* expression generally appears higher in wild-type embryos than in SU5402-treated embryos.

to the effects of heat shock at the 8-somite stage, pectoral fin formation appears to progress normally after heat shock at 24 hpf (SRM and DY, unpublished data). In an additional contrast to heat shock at the 8-somite stage, heat shock at 24 hpf only subtly affects heart morphology and looping (Figs. 5B, F) and does not affect ventricular or atrial cell number (Fig. 5G; Supplemental Table 5). Thus, our data suggest that, although ectopic FGF signaling at early stages can generate enlarged cardiomyocyte populations, this responsiveness to heightened FGF signaling is lost after the onset of myocardial differentiation.

Discussion

Our data demonstrate that FGF signaling plays an essential part in establishing the proper numbers and types of cardiomyocytes through a series of roles, beginning when myocardial progenitor specification is underway and continuing after the heart tube has formed. First, during gastrulation, FGF signaling promotes the formation of both ventricular and atrial lineages (Figs. 8A, B). Although atrial cell number does not depend on FGF signaling once gastrulation is complete, FGF signaling continues to promote development of the ventricular lineage while myocardial progenitor cells reside within the LPM (Figs. 8C, D). Even after the initiation of myocardial differentiation and the assembly of the heart tube, FGF signaling is important for the formation of the proper number of ventricular cardiomyocytes (Figs. 8E, F). Thus, reiterative roles of the FGF signaling pathway contribute to the regulation of both overall heart size and chamber proportionality.

Each of the temporally distinct roles of FGF signaling during establishment of cardiomyocyte populations correlates with the dynamic expression pattern of *fgf8*, in the sense that high levels of *fgf8* expression are located near the lineages affected by a loss of FGF signaling (Fig. 8). Moreover, given the similarities between the

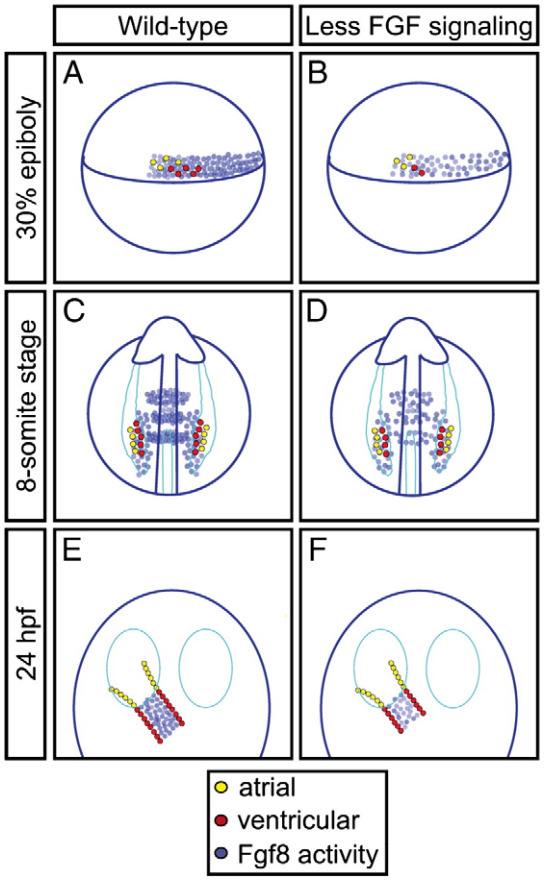

Fig. 8. FGF signaling plays reiterative roles in the establishment of heart size and chamber proportionality in zebrafish. (A–F) Schematics depict a model for the roles of FGF signaling indicated by our data. Each image represents the quantities of ventricular (red) or atrial (yellow) progenitor cells or cardiomyocytes and the locations of Fgf8 activity at the 30% epiboly stage (A, B, lateral views), the 8-somite stage (C, D, dorsal views), and 24 hpf (E, F, dorsal views), either in wild-type embryos (A, C, E) or in embryos with reduced FGF signaling (B, D, F). Locations of ventricular and atrial cells and Fgf8 activity in wild-type embryos are based on established fate map data and gene expression patterns (Auman et al., 2007; Fürthauer et al., 1997; Keegan et al., 2004; Reifers et al., 1998; Reifers et al., 2000; Schoenebeck et al., 2007). Differences depicted in (B, D, F) are inferred from the results presented here. (A, B) During gastrulation, FGF signaling along the margin influences both heart size and chamber proportionality by promoting specification or proliferation of myocardial progenitors, particularly ventricular progenitors. (C, D) During somitogenesis, FGF signaling near the medial LPM continues to influence ventricle proportion by promoting maintenance, proliferation, or differentiation of ventricular progenitors. (E, F) In the ventricular portion of the heart tube, FGF signaling influences ventricle proportion by regulating maintenance or augmentation of the ventricular cardiomyocyte population.

cardiac phenotypes of *ace* mutant embryos and embryos continuously treated with SU5402, it seems likely that Fgf8 is the major FGF family member with an influence on heart size and chamber proportionality in zebrafish. We cannot rule out the contribution of other FGFs, such as *fgf3* and *fgf24*, which are coexpressed with *fgf8* during gastrulation (Fürthauer et al., 2004); however, neither the *fgf3* nor *fgf24* mutant phenotypes are known to include cardiac defects (Fischer et al., 2003; Herzog et al., 2004). Hereafter, for simplicity of discussion, we refer to Fgf8 as the primary ligand of interest.

The temporally distinct effects of Fgf8 signaling on cardiomyocyte numbers provide suggestions for the cellular mechanisms responsible for establishing heart size and chamber proportionality. The early impact of Fgf8 signaling on heart size likely reflects a role of Fgf8 during the initial specification of ventricular and atrial myocardial progenitors or during the proliferation of these progenitors. During gastrulation stages, the multipotential mesendodermal progenitor cells that will ultimately give rise to the ventricular or atrial lineages are thought to be in the process of integrating the inductive signals that regulate their fate assignment (Brand, 2003; Zaffran and Frasch, 2002). Although our data do not address the cell autonomy of the requirement for receiving Fgf8 signaling, the known proximity of *fgf8* expression to the origins of myocardial progenitors indicates an opportunity for inductive signal reception by progenitor cells. Therefore, we propose that Fgf8 signaling helps to establish heart size in zebrafish by promoting the formation of a properly sized myocardial progenitor pool, consistent with the roles of FGF signaling during cardiac specification in *Drosophila* and *Ciona* (Davidson et al., 2006; Michelson et al., 1998).

Similar to its influence on heart size, the impact of Fgf8 signaling on chamber proportionality begins during gastrulation. The ventricular lineage is more sensitive than the atrial lineage to reduction of Fgf8 signaling during gastrulation, and the sensitivity of ventricular cells continues during somitogenesis and tube assembly, well beyond the sensitivity of the atrial population. The reiterative importance of Fgf8 signaling for establishment of ventricular cardiomyocyte numbers is consistent with the previously reported suggestion of a continuous requirement for Fgf8 signaling during zebrafish heart development (Reifers et al., 2000). Our data confirm and extend this prior work, providing a quantitative assessment of both ventricular and atrial cell number phenotypes in loss-of-function and gain-of-function scenarios at multiple stages.

Do the reiterative roles of FGF signaling in the establishment of chamber proportionality, like the role of FGF signaling in establishing heart size, reflect regulation of progenitor specification? During gastrulation and somitogenesis stages, the proximity of ventricular progenitors to the highest levels of *fgf8* expression (Figs. 8A, C) suggests an appealing model in which Fgf8 controls a ventricular/atrial fate decision: higher levels of Fgf8 signaling could induce ventricular identity, whereas lower levels of signaling could induce atrial identity. However, neither gastrulation treatment nor somitogenesis treatment with SU5402 leads to enhanced numbers of atrial cells, as would be expected if reduced Fgf8 signaling favored atrial specification over ventricular specification. Additionally, ectopic FGF signaling at the 8-somite stage leads to increases in both ventricular and atrial populations, instead of increasing the ventricular population at the expense of the atrial population. Therefore, although Fgf8 signaling may promote ventricular specification, particularly at gastrulation stages, its impact on chamber proportionality is more consistent with a particular influence on the ventricular lineage than with a role in regulating a binary decision between ventricular and atrial identities.

The comparison of FGF pathway loss-of-function and gain-of-function phenotypes during somitogenesis provides additional ideas for cellular mechanisms regulating ventricle proportion. Rather than reflecting a role in ventricular progenitor specification, the functions of Fgf8 signaling at these stages may indicate its importance for maintaining a population of ventricular progenitors, or for regulating the differentiation or proliferation of this population. These explanations fit well with the location of *fgf8* expression medially adjacent to the ventricular progenitor population (Fig. 8C). However, the ability of ectopic FGF signaling at the 8-somite stage to increase both the atrial and ventricular cardiomyocyte populations indicates an effect that extends beyond nurturing a population of ventricular progenitors. This expansion of both atrial and ventricular cells suggests that a degree of plasticity is retained in the LPM even after the initiation of *nkx2.5* expression, such that cell identity can still be swayed by high levels of FGF signaling.

Like reduction of Fgf8 signaling during somitogenesis, reduction of Fgf8 signaling after heart tube assembly results in a significant decrease in ventricular cell number but has no effect on atrial cell number. This is not likely to reflect a role of FGF signaling in promoting ventricular progenitor specification, since ectopic FGF signaling at 24 hpf is unable to increase the number of cardiomyocytes. Additionally, although cardiomyocyte proliferation would be an attractive mechanism for ventricular growth, the failure of ectopic FGF signaling to enhance cardiomyocyte cell number argues against its regulation of ventricular proliferation. Furthermore, we have detected very few proliferating cells with BrdU incorporation assays or with phospho-histone-3 immunohistochemistry in either wild-type or SU5402-treated cardiomyocytes between 24 and 48 hpf (SRM and DY, unpublished data). This is consistent with prior studies showing that, even though the number of cardiomyocytes increases by as much as 50% between 24 and 36 hpf (Rohr et al., 2006; Sato et al., 2006; Shu et al., 2003), the cardiomyocyte mitotic index is no greater than 10% during this time period (Rohr et al., 2006).

Instead of suggesting a late role of Fgf8 in ventricular specification or proliferation, our results point toward a role of Fgf8 in maintaining the proper number of differentiated ventricular cardiomyocytes, perhaps by promoting ventricular cardiomyocyte survival. However, TUNEL analysis of embryos treated with SU5402 during tube stages did not reveal an increase in apoptotic cardiomyocytes, and the ventricular cell number deficiency in *ace* mutant embryos is not ameliorated by treatment with caspase antagonists at tube stages (SRM and DY, unpublished data). Therefore, rather than invoking a role for Fgf8 in ventricular cardiomyocyte survival, it is interesting to consider another possibility, in which Fgf8 plays a role in the recruitment of additional cardiomyocytes into the heart tube after 24 hpf. Consistent with this model, tissue-specific *Fgf8* knockout mice have implicated Fgf8 in the regulation of proliferation and survival of progenitor cells within the anterior heart field, which contributes cardiomyocytes to the outflow pole after the formation of the primitive heart tube (Ilagan et al., 2006; Park et al., 2006). Perhaps Fgf8 signaling regulates the addition of cells from a secondary source to the outflow pole of the zebrafish heart, potentially by promoting their survival, differentiation, or migration. This secondary source could be the zebrafish equivalent to the amniote anterior heart field or, alternatively, might relate to the neural crest populations that have been suggested to contribute to the zebrafish myocardium (Li et al., 2003; Sato et al., 2006; Sato and Yost, 2003).

Taken together, our data suggest a model in which a single signaling pathway, and perhaps even a single growth factor, can act reiteratively to coordinate heart size and chamber proportionality. Fgf8 signaling acts early to create a cardiac progenitor pool of appropriate total size and ventricular/atrial proportionality. However, ventricle proportion is not regulated solely through generation of progenitor cells; it is also enforced by the continuing chamber-specific effects of Fgf8 that impact ventricular progenitor maintenance, ventricular differentiation, or recruitment of additional ventricular cardiomyocytes. The effects of FGF signaling extend even further into the more mature ventricle, in which FGFs influence ventricular growth, homeostasis, and regeneration (Lavine et al., 2005; Lepilina et al., 2006; Wills et al., 2008). In future studies, it will be important to

determine whether the same downstream effectors of FGF signaling are utilized in each temporal context and to elucidate how the FGF pathway networks with other pathways that contribute to myocardial specification, differentiation, and maintenance during the establishment of heart size and chamber proportionality.

Acknowledgments

We thank J. Schoenebeck for helpful observations and input, R. Friesel for sharing the *Xenopus* K562E construct, K. Rohr and J. Bakkers for reagents, J. Castro Lopes for support, and members of the Yelon laboratory for feedback. This work was supported by grants from the National Institutes of Health to DY and KDP. SRM received support from the GABBA Program and the Portuguese Foundation for Science and Technology (POCI 2010-FSE).

Appendix A. Supplementary data

Supplementary data associated with this article can be found, in the online version, at doi:10.1016/j.ydbio.2008.06.033.

References

Abu-Issa, R., et al., 2002. Fgf8 is required for pharyngeal arch and cardiovascular development in the mouse. Development 129, 4613–4625.
Ahn, D.G., et al., 2002. T-box gene tbx5 is essential for formation of the pectoral limb bud. Nature 417, 754–758.
Alsan, B.H., Schultheiss, T.M., 2002. Regulation of avian cardiogenesis by Fgf8 signaling. Development 129, 1935–1943.
Auman, H.J., Yelon, D., 2004. Vertebrate organogenesis: getting the heart into shape. Curr. Biol. 14, R152–153.
Auman, H.J., et al., 2007. Functional modulation of cardiac form through regionally confined cell shape changes. PLoS Biol. 5, e53.
Begemann, G., Ingham, P.W., 2000. Developmental regulation of Tbx5 in zebrafish embryogenesis. Mech. Dev. 90, 299–304.
Beiman, M., et al., 1996. Heartless, a *Drosophila* FGF receptor homolog, is essential for cell migration and establishment of several mesodermal lineages. Genes Dev. 10, 2993–3002.
Berdougo, E., et al., 2003. Mutation of weak atrium/atrial myosin heavy chain disrupts atrial function and influences ventricular morphogenesis in zebrafish. Development 130, 6121–6129.
Böttcher, R.T., Niehrs, C., 2005. Fibroblast growth factor signaling during early vertebrate development. Endocr. Rev. 26, 63–77.
Brand, T., 2003. Heart development: molecular insights into cardiac specification and early morphogenesis. Dev. Biol. 258, 1–19.
Brown, L.A., et al., 1998. Molecular characterization of the zebrafish PEA3 ETS-domain transcription factor. Oncogene 17, 93–104.
Cook, M., Tyers, M., 2007. Size control goes global. Curr. Opin. Biotechnol. 18, 341–350.
Crump, J.G., et al., 2004. An essential role for Fgfs in endodermal pouch formation influences later craniofacial skeletal patterning. Development 131, 5703–5716.
Davidson, B., et al., 2006. FGF signaling delineates the cardiac progenitor field in the simple chordate, *Ciona intestinalis*. Genes Dev. 20, 2728–2738.
Dell'Era, P., et al., 2003. Fibroblast growth factor receptor-1 is essential for in vitro cardiomyocyte development. Circ. Res. 93, 414–420.
Deng, C.X., et al., 1994. Murine FGFR-1 is required for early postimplantation growth and axial organization. Genes Dev. 8, 3045–3057.
Fischer, S., et al., 2003. The zebrafish fgf24 mutant identifies an additional level of Fgf signaling involved in vertebrate forelimb initiation. Development 130, 3515–3524.
Fürthauer, M., et al., 1997. A role for FGF-8 in the dorsoventral patterning of the zebrafish gastrula. Development 124, 4253–4264.
Fürthauer, M., et al., 2004. Fgf signalling controls the dorsoventral patterning of the zebrafish embryo. Development 131, 2853–2864.
Griffin, K.J., Kimelman, D., 2003. Interplay between FGF, one-eyed pinhead, and T-box transcription factors during zebrafish posterior development. Dev. Biol. 264, 456–466.
Hamade, A., et al., 2006. Retinoic acid activates myogenesis in vivo through Fgf8 signalling. Dev. Biol. 289, 127–140.
Herzog, W., et al., 2004. Fgf3 signaling from the ventral diencephalon is required for early specification and subsequent survival of the zebrafish adenohypophysis. Development 131, 3681–3692.
Hidalgo, A., ffrench-Constant, C., 2003. The control of cell number during central nervous system development in flies and mice. Mech. Dev. 120, 1311–1325.
Higashijima, S., et al., 1997. High-frequency generation of transgenic zebrafish which reliably express GFP in whole muscles or the whole body by using promoters of zebrafish origin. Dev. Biol. 192, 289–299.
Ilagan, R., et al., 2006. Fgf8 is required for anterior heart field development. Development 133, 2435–2445.
Keegan, B.R., et al., 2004. Organization of cardiac chamber progenitors in the zebrafish blastula. Development 131, 3081–3091.
Kurita, R., et al., 2003. Suppression of lens growth by alphaA-crystallin promoter-driven expression of diphtheria toxin results in disruption of retinal cell organization in zebrafish. Dev. Biol. 255, 113–127.
Lavine, K.J., et al., 2005. Endocardial and epicardial derived FGF signals regulate myocardial proliferation and differentiation in vivo. Dev. Cell. 8, 85–95.
Lepilina, A., et al., 2006. A dynamic epicardial injury response supports progenitor cell activity during zebrafish heart regeneration. Cell. 127, 607–619.
Linzbach, A., 1960. Heart failure from the point of view of quantitative anatomy. Am. J. Cardiol. 370–382.
Li, Y.X., et al., 2003. Cardiac neural crest in zebrafish embryos contributes to myocardial cell lineage and early heart function. Dev. Dyn. 226, 540–550.
Lopez-Sanchez, C., et al., 2002. Induction of cardiogenesis by Hensen's node and fibroblast growth factors. Cell Tissue Res. 309, 237–249.
Mably, J.D., et al., 2003. Heart of glass regulates the concentric growth of the heart in zebrafish. Curr. Biol. 13, 2138–2147.
Maroon, H., et al., 2002. Fgf3 and Fgf8 are required together for formation of the otic placode and vesicle. Development 129, 2099–2108.
Mercader, N., et al., 2006. Prdm1 acts downstream of a sequential RA, Wnt and Fgf signaling cascade during zebrafish forelimb induction. Development 133, 2805–2815.
Michelson, A.M., et al., 1998. Dual functions of the heartless fibroblast growth factor receptor in development of the *Drosophila* embryonic mesoderm. Dev. Genet. 22, 212–229.
Mohammadi, M., et al., 1997. Structures of the tyrosine kinase domain of fibroblast growth factor receptor in complex with inhibitors. Science 276, 955–960.
Nechiporuk, A., et al., 2005. Endoderm-derived Fgf3 is necessary and sufficient for inducing neurogenesis in the epibranchial placodes in zebrafish. Development 132, 3717–3730.
Neilson, K.M., Friesel, R., 1996. Ligand-independent activation of fibroblast growth factor receptors by point mutations in the extracellular, transmembrane, and kinase domains. J. Biol. Chem. 271, 25049–25057.
Nijhout, H.F., 2003. The control of body size in insects. Dev. Biol. 261, 1–9.
Nusslein-Volhard, C., Dahm, R., 2002. Zebrafish, A Practical Approach. Oxford University Press.
Park, E.J., et al., 2006. Required, tissue-specific roles for Fgf8 in outflow tract formation and remodeling. Development 133, 2419–2433.
Potter, C.J., Xu, T., 2001. Mechanisms of size control. Curr. Opin. Genet. Dev. 11, 279–286.
Raff, M.C., 1996. Size control: the regulation of cell numbers in animal development. Cell. 86, 173–175.
Reifers, F., et al., 1998. Fgf8 is mutated in zebrafish acerebellar (ace) mutants and is required for maintenance of midbrain–hindbrain boundary development and somitogenesis. Development 125, 2381–2395.
Reifers, F., et al., 2000. Induction and differentiation of the zebrafish heart requires fibroblast growth factor 8 (fgf8/acerebellar). Development 127, 225–235.
Roehl, H., Nüsslein-Volhard, C., 2001. Zebrafish pea3 and erm are general targets of FGF8 signaling. Curr. Biol. 11, 503–507.
Rohr, S., et al., 2006. Heart and soul/PRKCi and nagie oko/Mpp5 regulate myocardial coherence and remodeling during cardiac morphogenesis. Development 133, 107–115.
Sato, M., Yost, H.J., 2003. Cardiac neural crest contributes to cardiomyogenesis in zebrafish. Dev. Biol. 257, 127–139.
Sato, M., et al., 2006. Semaphorin3D regulates invasion of cardiac neural crest cells into the primary heart field. Dev. Biol. 298, 12–21.
Schoenebeck, J.J., et al., 2007. Vessel and blood specification override cardiac potential in anterior mesoderm. Dev. Cell. 13, 254–267.
Shu, X., et al., 2003. Na,K-ATPase is essential for embryonic heart development in the zebrafish. Development 130, 6165–6173.
Stainier, D.Y., et al., 1993. Cardiovascular development in the zebrafish. I. Myocardial fate map and heart tube formation. Development 119, 31–40.
Sun, X., et al., 1999. Targeted disruption of Fgf8 causes failure of cell migration in the gastrulating mouse embryo. Genes Dev. 13, 1834–1846.
Trumpp, A., et al., 2001. c-Myc regulates mammalian body size by controlling cell number but not cell size. Nature 414, 768–773.
Wills, A.A., et al., 2008. Regulated addition of new myocardial and epicardial cells fosters homeostatic cardiac growth and maintenance in adult zebrafish. Development 135, 183–192.
Yelon, D., et al., 1999. Restricted expression of cardiac myosin genes reveals regulated aspects of heart tube assembly in zebrafish. Dev. Biol. 214, 23–37.
Yelon, D., et al., 2000. The bHLH transcription factor hand2 plays parallel roles in zebrafish heart and pectoral fin development. Development 127, 2573–2582.
Zaffran, S., Frasch, M., 2002. Early signals in cardiac development. Circ. Res. 91, 457–469.
Zhu, X., et al., 1999. Evidence that FGF receptor signaling is necessary for endoderm-regulated development of precardiac mesoderm. Mech. Ageing Dev. 108, 77–85.